High-Field Electrical Transport in Single-Wall Carbon Nanotubes

Zhen Yao,[1] Charles L. Kane,[2] and Cees Dekker[1]

[1]*Department of Applied Physics and DIMES, Delft University of Technology, Lorentzweg 1, 2628 CJ Delft, The Netherlands*
[2]*Department of Physics, University of Pennsylvania, Philadelphia, Pennsylvania 19104*

(Received 5 November 1999)

Using low-resistance electrical contacts, we have measured the intrinsic high-field transport properties of metallic single-wall carbon nanotubes. Individual nanotubes appear to be able to carry currents with a density exceeding 10^9 A/cm^2. As the bias voltage is increased, the conductance drops dramatically due to scattering of electrons. We show that the current-voltage characteristics can be explained by considering optical or zone-boundary phonon emission as the dominant scattering mechanism at high field.

PACS numbers: 73.50.Fq, 72.10.Di, 73.61.Wp

The potential electronic application of single-wall carbon nanotubes (SWNTs) requires a detailed understanding of their fundamental electronic properties, which are particularly intriguing due to their one-dimensional (1D) nature [1]. Metallic SWNTs have two 1D subbands crossing at the Fermi energy. In the ideal case the resistance is thus predicted to be $h/4e^2$ or 6.5 kΩ. In early electrical transport experiments, however, the nanotubes typically formed a tunnel barrier of high resistance of $\sim$1 MΩ with the metal contacts [2,3]. Consequently, the bias voltage dropped almost entirely across the contacts, and tunneling dominated the transport. A number of interesting phenomena have been observed in this regime. At low temperatures, Coulomb blockade effects prevail [2,3]. At relatively high temperatures, the transport characteristics appear to be described by tunneling into the so-called Luttinger liquid—a unique correlated electronic state in 1D conductors which is due to electron interactions [4,5].

One of the most important questions that remains to be addressed is how the electrons traverse the nanotubes, i.e., whether ballistically or being scattered by impurities or phonons. The unusual band structure of metallic tubes suggests a suppression of elastic backscattering of electrons by long-range disorder [6]. Long mean-free paths for electrons near the Fermi energy have indeed been inferred from regular Coulomb oscillations and coherent tunneling at low temperatures [2,7]. However, there has been no transport study of electrons with significant excess energy above the Fermi energy. It is not clear whether such electrons would experience strong scattering and what type of scattering mechanism would dominate.

In this Letter we present electrical transport measurements of individual nanotubes using low-resistance contacts (LRCs). In contrast to the high-resistance contacts (HRCs), a bias voltage applied between two LRCs establishes an electric field across the nanotube which accelerates the electrons, enabling transport studies of high-energy electrons. We find that individual SWNTs can sustain a remarkably high current density of more than 10^9 A/cm^2. The current seems to saturate at high electric field. We discuss possible scattering mechanisms and suggest that optical or zone-boundary phonon emission by high-energy electrons can explain the observed behavior. An analytic theory based on the Boltzmann equation is developed which includes both elastic scattering and phonon emission. The numerical calculations reproduce the experimental results remarkably well.

The inset of Fig. 1(a) shows an atomic force microscope (AFM) image of our typical LRC sample. The 20 nm thick, 250 nm wide Ti/Au electrodes are embedded in thermally grown SiO_2 with a height difference of less than 1 nm which minimizes the deformation of the nanotubes near the electrodes. This is achieved by electron-beam lithography and anisotropic reactive-ion etching of SiO_2 using a single layer of polymethylmethacrylate as both

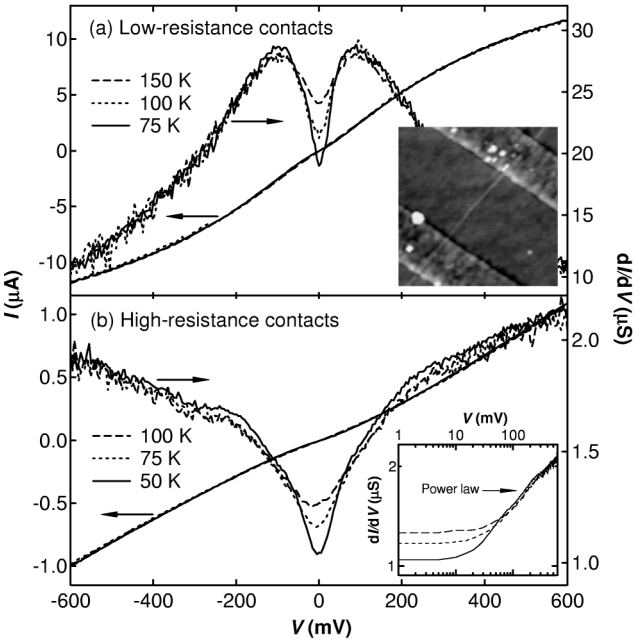

FIG. 1. Typical I and dI/dV vs V obtained using (a) low- and (b) high-resistance contacts. The inset to (a) shows a 0.86 $\times$ 0.86 μm^2 AFM height image of a typical LRC sample, where the z range is 10 nm. The inset to (b) plots dI/dV vs V on a double-log scale for the HRC sample.

electron-beam resist and etching mask, followed by metal evaporation and lift-off. The electrodes are cleaned thoroughly in fuming nitric acid. The nanotubes are then deposited on top of the electrodes from a suspension of SWNTs ultrasonically dispersed in dichloroethane. We find that brief annealing of the electrodes at 180 °C improves the reproducibility of the contact resistance. Only nanotubes with apparent height of $\sim$1 nm under AFM are chosen for transport measurements, which are presumably individual SWNTs. Metallic nanotubes are selected based on the absence of gate effect on transport at high temperatures [8]. This procedure yields a typical two-terminal resistance of individual metallic tubes of less than 100 kΩ (the lowest is 17 kΩ) at room temperature, as compared to the $\sim$MΩ resistance using Pt as the contact material in previous experiments [2]. Similar reduction in contact resistance has also been achieved in a different contact geometry [9]. The exact mechanism for the low contact resistance is unclear. However, clean flat gold facets may increase the coupling by increasing the effective contact length with a small tube-electrode separation [10].

Figure 1 shows the typical two-terminal current I and differential conductance dI/dV vs voltage V obtained using LRC (Au) and HRC (Pt). dI/dV is acquired simultaneously using a standard ac lock-in technique. The room-temperature zero-bias resistance of the two samples are 40 and 670 kΩ, respectively. For both samples, the zero-bias conductance G decreases monotonically as the temperature T decreases [11]. The large-bias-voltage dependence of dI/dV, however, is notably different. For the LRC sample, dI/dV increases with increasing bias, reaching a maximum at $\sim$100 mV. As the bias increases further, dI/dV drops dramatically. In contrast, the HRC sample exhibits a monotonic increase of dI/dV as a function of voltage up to 1 V. The inset of Fig. 1(b) plots dI/dV vs V on a double-logarithmic scale for the HRC sample, in which it appears that dI/dV can be fit with a power-law function for large bias. Both the temperature dependence of G and the bias-voltage dependence of dI/dV for the HRC sample are typical of individual SWNTs and ropes with similar or lower conductance values [4], which are attributed to the suppressed tunneling density of states in a Luttinger liquid [12]. The similar behavior around zero bias for the LRC sample suggests that it comes from the same origin. In the remainder of the paper, we focus on the large-bias behavior for the LRC samples.

We have further extended the I-V measurements up to 5 V as shown in Fig. 2. Strikingly, the I-V curves at large bias measured at different temperatures between 4 K and room temperature essentially overlap with each other. The current at 5 V exceeds 20 μA, which corresponds to a current density of more than 10^9 A/cm^2 if a spatial extent of the π-electron orbital of $\sim$3 Å is used to estimate the current-carrying cross section. From the shape of the I-V curves, it is clear that the trend of decreasing conductance

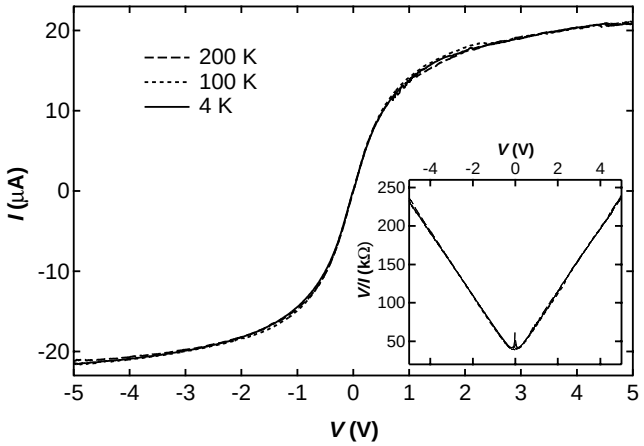

FIG. 2. Large-bias I-V characteristics at different temperatures using low-resistance contacts for a sample with an electrode spacing of 1 μm. The inset plots $R \equiv V/I$ vs V.

continues to high bias. Extrapolating the measured I-V curves to higher voltage would lead to a current saturation, i.e., a vanishing conductance. Interestingly, the saturation current seems to be independent of the distance between the electrodes [13].

We find that the resistance, $R \equiv V/I$, can be fit remarkably well by a simple linear function of V over almost the entire range of applied voltage (see Fig. 2, inset),

$$R = R_0 + V/I_0, \tag{1}$$

where R_0 and I_0 are constants. Only at high voltages near 5 V some samples start showing slight deviation from this linear behavior. From the slope of the linear part of R-V we find $I_0 \sim 25$ μA which is approximately the same for all of the samples we have measured.

At first sight the current saturation might be explained from the band structure. Current in metallic nanotubes is carried by two propagating 1D subbands. In the absence of scattering, the chemical potentials of the right and left moving states will differ by the applied voltage eV. At low voltages this leads to an Ohmic response, but when eV exceeds the Fermi energy of the 1D subbands, the left moving states will be completely depleted and the current will saturate. The Fermi energy, measured relative to the nearest band edge, is approximately 2.9 eV. Experimentally, however, the current starts saturating at a much lower voltage. An alternative model is thus needed to explain the saturation.

We expect the measured resistance to be a combination of the resistance due to the contacts and the resistance due to backscattering along the length of the nanotube. The current saturation is unlikely to arise from an increased contact resistance at high voltages since the contacts would then behave like high-resistance tunneling contacts, and one would expect to see features in the I-V associated with tunneling into the 1D subbands of the nanotube. The measured I-V, however, is featureless.

We thus focus on the effect of backscattering in the nanotube. The behavior of R-V suggests that in addition to a constant scattering term, which most probably comes from contact scattering or impurity scattering, there is a dominant scattering mechanism with a mean free path (mfp) which scales inversely with the voltage.

Electrons can backscatter off phonons and other electrons. Electron-electron scattering is appealing at first, since it does not involve heating the lattice. The only electron-electron scattering that contributes to resistivity is umklapp scattering [14] with a scattering rate directly proportional to the electron temperature T_e. This gives $V/I \sim T_e$. T_e will be determined by how fast the heat can escape from the tube. If we assume that all the heat produced is carried by electrons into the leads and that the temperature along the tube is uniform [15], we have $IV = 4(\pi^2/3)(k_B T_e)^2/h$, where the left-hand side is the rate at which heat is produced, and the right-hand side is the heat current carried by the two 1D channels. Hence we expect that $I \sim V^{1/3}$, which cannot describe the experiments. We have verified this $V^{1/3}$ behavior by numerically solving a Boltzmann equation similar to that discussed below. Luttinger-liquid effects, which have been ignored in the above arguments, tend to enhance umklapp scattering at low energies [12]. This would make the agreement with experiment even worse.

This suggests that we must consider scattering from phonons. The coupling will be strongest for phonons which compress and stretch bonds on the lattice scale. There are three possible categories of phonons: (1) twistons or long-wavelength acoustic phonons [16], (2) optical phonons which are derived from the in-plane E_{2g_2} mode of graphite with a frequency of 1580 cm^{-1}, and (3) in-plane zone-boundary phonons with momentum which connects the two Fermi points of graphene. While zone-boundary phonons are not directly observable optically, force-constant models put their frequency in the range 1000–1500 cm^{-1} [17]. Twiston scattering is not relevant. The mfp for twiston scattering was estimated in [16] using a simple tight-binding model for the electron-phonon coupling. Comparing this with a corresponding estimate of the optical phonon scattering mfp shows that the optical phonon scattering dominates, provided $T \ll \Theta_D \ll eV/k_B$ ($\Theta_D \sim 2000$ K is the Debye temperature). Moreover, twistons may be pinned by the substrate.

Now we discuss backscattering due to the emission of optical or zone-boundary phonons. A related effect has been discussed previously in the context of semiconductors [18]. The key point is that for an electron with energy E to emit a phonon of energy $\hbar\Omega$, there must be an available state to scatter into at energy $E - \hbar\Omega$. In the presence of an electric field $\mathcal{E}$, electrons are accelerated, $\hbar\dot{k} = e\mathcal{E}$. It is simplest to consider the case in which the coupling to the phonon is so strong that, once an electron reaches the threshold for phonon emission, it is immediately backscattered. As indicated in the schematic in the inset of Fig. 3, a steady state population is then established in which the right moving electrons are populated to an energy $\hbar\Omega$ higher than the left moving ones. The current carried in this state can be computed from a Landauer type argument to be

$$I_0 = (4e/h)\hbar\Omega\,. \tag{2}$$

If we choose $\hbar\Omega = 0.16$ eV (corresponding to 1300 cm^{-1}), this leads to a saturation current of 25 μA, which is independent of sample length and agrees very well with the measured saturation current.

In this picture, the mfp for backscattering phonons ℓ_Ω is equal to the distance an electron must travel to be accelerated to an energy above the phonon energy: $\ell_\Omega = \hbar\Omega/e\mathcal{E}$. This may be combined with a constant elastic scattering term via Mathiessen's rule to obtain an effective mfp, $\ell_{\rm eff}^{-1} = \ell_e^{-1} + \ell_\Omega^{-1}$, where ℓ_e is the elastic scattering mfp. The resulting resistance, $R = (h/4e^2)(L/\ell_{\rm eff})$, then has the empirically observed form of Eq. (1) with $R_0 = (h/4e^2)L/\ell_e$ and I_0 given in Eq. (2).

To put the above interpretation on a more quantitative basis, we consider the Boltzmann equation for the distribution functions $f_{L,R}(E_k, x, t)$ of left and right moving (L, R) electrons (details will be provided in a future publication):

$$[\partial_t \pm v_F\partial_x \pm v_F e\mathcal{E}\,\partial_E] f_{L,R} = [\partial_t f_{L,R}]_{\rm col}\,. \tag{3}$$

Here v_F is the Fermi velocity, and we have chosen to express the momentum dependence of f in terms of $E_k = \pm\hbar v_F k$. The left-hand side describes the collisionless evolution of the electrons in the presence of an electric field $\mathcal{E}$. For the collision term on the right, we consider a sum of three terms: (1) Elastic scattering, $[\partial_t f_L]_e = (v_F/\ell_e)(f_R - f_L)$, where ℓ_e is the elastic mfp. (2) Backscattering from phonons, $[\partial_t f_L]_{\rm pb} = (v_F/\ell_{\rm pb})[(1 - f_L)f_R^+ - f_L(1 - f_R^-)]$. Here

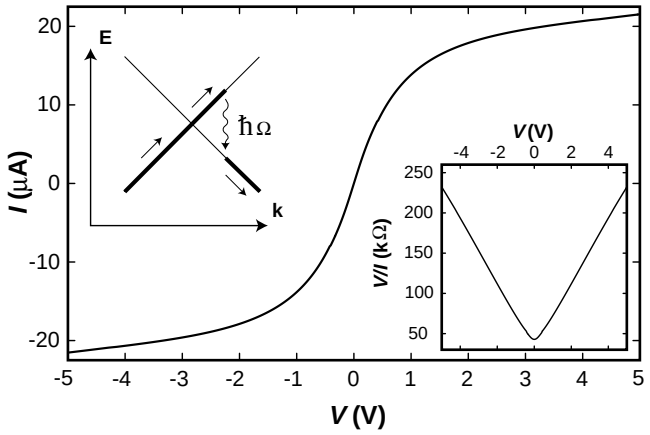

FIG. 3. Numerical calculation of I-V characteristic by solving Boltzmann transport equation including elastic impurity scattering and phonon emission as depicted in the left inset. See text for the parameters used.

$f^{\pm}$ are evaluated at $E \pm \hbar\Omega$. $\ell_{\rm pb}$, which depends on the strength of the electron-phonon coupling, is the distance an electron travels before backscattering once the phonon emission threshold has been reached. This should be contrasted with ℓ_Ω, the distance required to reach the threshold. We assume that the phonon temperature is much less than the phonon energy of $\sim$2000 K, so that the Bose occupation factors can be ignored. Finally, we consider (3) forward scattering from phonons, $[\partial_t f_L]_{\rm pf} = (v_F/\ell_{\rm pf})[(1 - f_L)f_L^+ - f_L(1 - f_L^-)]$.

The effects of the contact resistance may be included as a boundary condition at the ends of the tube. For instance, at the left contact ($x = 0$) we have

$$f_R(E,0) = t_L^2 f_0(E - \mu_L) + (1 - t_L^2) f_L(E,0), \quad (4)$$

where t_L^2 is the transmission probability for the contact, and $f_0(E - \mu_L) = \{\exp[(E - \mu_L)/k_{\rm B}T] + 1\}^{-1}$ is the Fermi distribution function of the left contact with electrochemical potential μ_L and temperature T.

We have solved Eqs. (3) and (4) numerically to obtain the steady state distribution function $f_{L,R}(E,x)$ in the presence of an applied voltage $\mu_L - \mu_R = eV$ as a function of $\hbar\Omega$, $\ell_{\rm e}$, $\ell_{\rm pb,pf}$, and $t_{L,R}^2$. The current is then simply given by $I = (4e/h)\int dE(f_L - f_R)$. Figure 3 shows an example of the numerical calculation of I-V characteristic for a sample length of $L = 1$ μm. The parameters used in the plot are $\hbar\Omega = 0.15$ eV, $t_{L,R}^2 = 0.5$, $\ell_{\rm e} = 300$ nm, $\ell_{\rm pb} = 10$ nm, and $\ell_{\rm pf} = \infty$. The resemblance to the experiment is remarkable. It is interesting to note that the current is insensitive to the contact scattering for $V \gtrsim 0.5$ V. Contact scattering affects only the low bias resistance, giving rise to the positive curvature in R-V near $V = 0$.

Assuming local thermal equilibrium, the Boltzmann equation may be used to derive hydrodynamic equations which govern the transport of charge and energy. These equations may then be solved analytically and give results which agree well with the simulations. They show the following: (i) The empirical formula [Eq. (1)] is exact in the limit $eV \ll \hbar\Omega L/\ell_{\rm pb}$, which means that the energy gained by an electron within distance $\ell_{\rm pb}$ must be much less than the phonon energy, or, equivalently, $\ell_{\rm pb} \ll \ell_\Omega$. (ii) For larger V the simple formula breaks down, and in the limit of very large V the resistance becomes constant, $R = (h/4e^2)L(\ell_{\rm e}^{-1} + \ell_{\rm pb}^{-1})$. For the parameters used in Fig. 3, the crossover voltage is roughly 15 eV. Indeed, there appears a small negative curvature at 5 V in the V/I vs V plot (inset of Fig. 3), which signals the beginning of the breakdown of the empirical formula. The curvature would be less pronounced if a shorter value for $\ell_{\rm pb}$ is used. We note that 10 nm seems rather short. An estimate using a simple tight-binding model gives $\ell_{\rm pb} \sim 100$ nm. More work is needed to have a more accurate estimate of the electron-phonon coupling strength.

We have assumed that the heat generated in the tube escapes sufficiently quickly to avoid raising the lattice temperature too high. A simple estimate of the nanotube's thermal conductivity indicates that it is unlikely that all of the heat could be transmitted through the contacts. However, the nanotube is in intimate contact along its entire length with the substrate, which may be regarded as a thermal reservoir. It would clearly be desirable to study further the nature of the thermal contact between the nanotube and substrate. Measurements on suspended nanotubes may provide some useful information.

We thank R. E. Smalley and co-workers for providing the indispensable nanotube materials, M. P. Anantram, H. Postma, and S. J. Tans for discussions, and A. van den Enden for technical assistance. The work at Delft was supported by the FOM and the work at Pennsylvania by the NSF under Grant No. DMR 96-32598.

[1] C. Dekker, Phys. Today **52**, No. 5, 22 (1999).
[2] S. J. Tans *et al.,* Nature (London) **386**, 474 (1997).
[3] M. Bockrath *et al.,* Science **275**, 1922 (1997).
[4] M. Bockrath *et al.,* Nature (London) **397**, 598 (1999); H. Postma *et al.* (unpublished).
[5] Z. Yao, H. Postma, L. Balents, and C. Dekker, Nature (London) **402**, 273 (1999).
[6] T. Ando, T. Nakanishi, and R. Saito, J. Phys. Soc. Jpn. **67**, 1704 (1997).
[7] P. L. McEuen *et al.,* Phys. Rev. Lett. **83**, 5098 (1999).
[8] S. J. Tans, A. R. M. Verschueren, and C. Dekker, Nature (London) **393**, 49 (1998).
[9] H. T. Soh *et al.,* Appl. Phys. Lett. **75**, 627 (1999).
[10] J. Tersoff, Appl. Phys. Lett. **74**, 2122 (1999); M. P. Anantram, S. Datta, and Y. Xue, cond-mat/9907357.
[11] We have also observed an increasing conductance as temperature decreases for those samples with a two-probe resistance of less than 25 kΩ at room temperature, similar to that found in Ref. [9].
[12] R. Egger and G. Gogolin, Phys. Rev. Lett. **79**, 5082 (1997); C. L. Kane, L. Balents, and M. P. A. Fisher, *ibid.* **79**, 5086 (1997).
[13] The current at 5 V for different samples varies between 19 and 23 μA with a variation in electrode spacing between 700 nm and 2 μm.
[14] L. Balents and M. P. A. Fisher, Phys. Rev. B **55**, 11 973 (1997).
[15] The temperature is uniform when the system is effectively at half filling across the length of the tube.
[16] C. L. Kane and E. J. Mele, Phys. Rev. Lett. **78**, 1932 (1997); C. L. Kane *et al.,* Europhys. Lett. **41**, 683 (1998).
[17] M. S. Dresselhaus, G. Dresselhaus, and P. C. Eklund, *Science of Fullerenes and Carbon Nanotubes* (Academic, San Diego, 1996).
[18] G. D. Mahan and G. S. Canright, Phys. Rev. B **35**, 4365 (1987).